Phaiie-Dispersion of Nonlinear Optical Susceptibilities

Cid B. de Araújo, H. Ma, A. S. L. Gomes and L. H. Acioli
Departamento de *Física,* Universidade Federal de Pernambuco
50739 Recife, Brasil

Received November 26, 1992

New methods for measuring the phase-dispersion of the third- and fifth-order susceptibilities cre reviewed. The measurements were based on the phenomenon of polarization beats which was exploited in time-delayed wave-mixing experiments with bichromatic beams. Applications for semiconductor doped glasses are reported.

I. Introduction

Studies o[r] the phase-dispersion of nonlinear optical susceptibilities have proved to be helpful to characterize the naturr of the nonlinearity as well as to improve material's properties along the past three decades[1,2]. A variety of methods are presently available to determine the phase of the second-order susceptibility, $\chi^{(2)}$, through seccnd-harmonic and sum-frequency generation spectroscopy[3–6]. The phase-dispersion of third-order susceptibilities, $\chi^{(3)}$, has been measured, for example, in four-wave-mixing experiments by investigating resonance interferences among the various $\chi^{(3)}$ contributions[3,7], by producing interferences with the signal generated by a reference sample[8,9] or using interferometric and absorptive techniques[3,7]. In general these methods allow the study of degenerate (or quasi-degenerate) $\chi^{(3)}$. On the other hand, the phase of non-degenerate $\chi^{(3)}$ may be deterrnined using a combination of techniques which may provide values for $|\chi^{(3)}|$, $Re\chi^{(3)}$ and $Im\chi^{(3)}$ in separate experiments. These measurements have been performed in the past twenty years but were limited to frequency values which do not differ by a large amount[3,7,10–12]. The situation is worse for high-order susceptibilities ($\chi^{(5)}, \chi^{(7)}, ...$) since no technique for measuring phases has been reported in the past.

Recently, the polarization beats phenomena[13–16] has been successfully exploited to measure phases of nondegenerate $\chi^{(3)}$ and $\chi^{(5)}$ in a variety of conditions[17–20]. In principle, when combining these techniques with the "two-color z-scan method"[21,22] it is possible to characterize the nondegenerate susceptibility of nonlinear materials in a large range of optical frequencies. These measurements may provide basic information cn the physical mechanisms contributing to the optical susceptibility. From a practical point of view, knowledge of nondegenerate susceptibility is of interest for dual-wavelength all-optical switching applications in which cross-phase modulation (XPM) plays an essential role. On the other hand, XPM processes may also allow beam profile manipulations in a variety of situations of fundamental interest (see for example refs. [23-26]).

In this paper we review our own recent work in this area and present further details that were not given in the previous publications.

II. Interferometry based on the polarization beats phenomenon

We describe in this section the observation of polarization beats induced via $\chi^{(3)}$ and $\chi^{(5)}$ and exploit this effect to measure the phases of both susceptibilities. The method presented here is quite general and can be applied for a large variety of materials for which forward-wave-mixing (self-diffraction) can be observed. To illustrate the method we measured the phases of $\chi^{(3)}$ and $\chi^{(5)}$ using samples of $Cd(S,Se)$ doped glasses. We start by giving a theoretical description necessary to understand the experiments.

a. Phase dispersion of $\chi^{(3)}$

First consider the beams geometry indicated in Fig.1 where each beam contains two frequencies, ω_1 and ω_2, with electric fields given by $E_i^{(j)}(\vec{r},t) = E_i^{(j)}\ exp\{i(\vec{k}_i^{(j)} \cdot \vec{r} - \omega_i t + \theta_i)\}$, i $= 1,2$, with parallel polarizations. $j = 1,2$ refer to the beams directions. The fields that interact in the sample are a combination of $E_1^{(j)}$ and $E_2^{(j)}$ such that diffracted beams can be emitted along both sides of the sample in various diffraction orders. Each emitted beam has frequency components ω_1 and ω_2. The signals along the directions $(2\vec{k}^{(1)} - \vec{k}^{(2)})$ and $(2\vec{k}^{(2)} - \vec{k}^{(1)})$ are due primarily to the third-order nonlinearity.

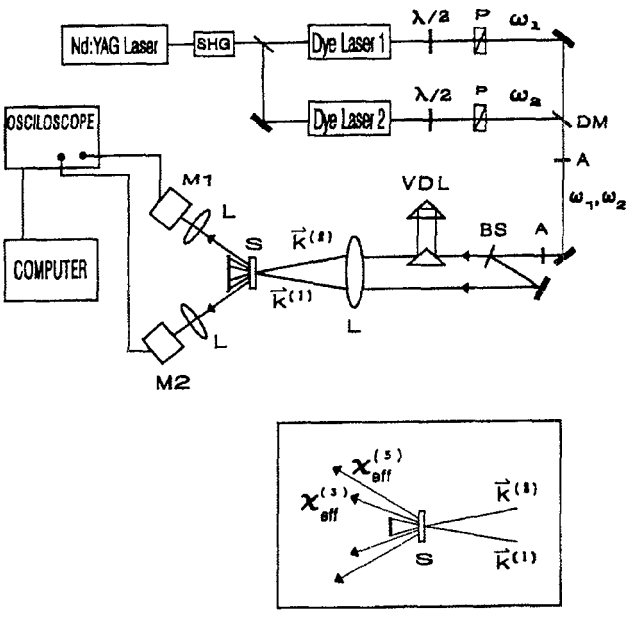

Figure 1: Experimental arrangement. $\lambda/2$ are half-wave plates and P are Glan-Thompson polanzers used in conjunction to adjust the laser power. A: apertures; BS: beam splitter; DM: dichroic mirror; VDL: variable delay line; L: convex lenses; M1 and M2 are $0.25m$ monochromators. The apertures are essential to reduce the background noise.

The signal beam at frequency ω_1 ernitted along $(2\vec{k}^{(1)} - \vec{k}^{(2)})$ is generated by the nonlinear polarization $P^{(3)}(\omega_1) = P_A^{(3)}(\omega_1) + P_B^{(3)}(\omega_1)$ with

$$P_A^{(3)}(\omega_1) = \chi^{(3)}(\omega_1,\omega_1,\omega_1,-\omega_1)E_1^{(1)}E_1^{(1)}E_1^{*(2)} \times \exp\{i\left[(2\vec{k}_1^{(1)} - \vec{k}_1^{(2)})\cdot\vec{r} - \omega_1 t + \omega_1\tau + \theta_1\right]\}, \quad (1)$$

and

$$P_B^{(3)}(\omega_1) = \chi^{(3)}(\omega_1,\omega_1,\omega_2,-\omega_2)E_1^{(1)}E_2^{(1)}E_2^{*(2)} \times \exp\left\{i\left[(\vec{k}_1^{(1)} + \vec{k}_2^{(1)} - \vec{k}_2^{(2)})\cdot\vec{r} - \omega_1 t + \omega_2\tau + \theta_1\right]\right\}, \quad (2)$$

where τ is the relative time delay between the two bichromatic beams.

The signal intensity at frequency ω_1 is proportional to $|P^{(3)}(\omega_1)|^2$ and is given by

$$I(\omega_1) \propto \left\{a^2 + b^2 + 2ab\cos\left[\Delta\vec{k}\cdot r + \omega_M\tau - \phi_1\right]\right\}, \quad (3)$$

where $a^2 = |\chi^{(3)}(\omega_1,\omega_1,\omega_1,-\omega_1)|^2 I_1^3$; $b^2 = |\chi^{(3)}(\omega_1,\omega_1,\omega_2,-\omega_2)|^2 I_1 I_2^2$; $\omega_M = \omega_1 - \omega_2$ is the modulation frequency which can be changed continuously and $\Delta\vec{k} = (\vec{k}_1^{(1)} - \vec{k}_2^{(1)}) - (\vec{k}_1^{(2)} - \vec{k}_2^{(2)})$. The signal modulation depth can be adjusted by changing the lasers' relative intensities.

The phase ϕ_1 depends on the material susceptibilities, being determined by

$$= arc\,\mathrm{tg}\left[\frac{Im\chi^{(3)}(\omega_1,\omega_1,\omega_2,-\omega_2)}{Re\,\chi^{(3)}(\omega_1,\omega_1,\omega_2,-\omega_2)}\right] - \mathrm{arctg}\left[\frac{Im\chi^{(3)}(\omega_1,\omega_1,\omega_1,-\omega_1)}{Re\,\chi^{(3)}(\omega_1,\omega_1,\omega_1,-\omega_1)}\right]. \quad (4)$$

Analogous calculations for $I(\omega_1)$ emitted along the direction $(2\vec{k}^{(2)} - \vec{k}^{(1)})$ provide a rnodulated signal $(+2\phi_1)$ out-of-phase with the signal indicated in Eq.(3). Consequently, if the signals in both directions are simultaneously recorded in two independent detectors, the absolute value of ϕ_1 can be measured. Furthermore, if one chooses the appropriate laser wavelengths to cancel one of the terms on the right hand side of eq.(4), the value of the other term can be determined. As will be shown latter, this can be done, for example, by selecting one laser frequency to be far from resonances.

For the signal component at frequency ω_2 it is possible to obtain an expression for $I(\omega_2)$ emitted along $(2\vec{k}^{(1)} - \vec{k}^{(2)})$ and $(2\vec{k}^{(2)} - \vec{k}^{(1)})$ directions using a procedure analogous to the one described above. In this case the susceptibilities which contribute for the signal are $\chi^{(3)}(\omega_2,\omega_2,\omega_2,-\omega_2)$ and $\chi^{(3)}(\omega_2,\omega_1,\omega_2,-\omega_1)$ and the corresponding phase of the signal is given by

$$\phi_2 = arc\,\mathrm{tg}\left[\frac{Im\chi^{(3)}(\omega_2,\omega_1,\omega_2,-\omega_1)}{Re\,\chi^{(3)}(\omega_2,\omega_1,\omega_2,-\omega_1)}\right] - \mathrm{arctg}\left[\frac{Im\chi^{(3)}(\omega_2,\omega_2,\omega_2,-\omega_2)}{Re\,\chi^{(3)}(\omega_2,\omega_2,\omega_2,-\omega_2)}\right]. \quad (5)$$

The experimental setup used is shown in Fig.1. The dye lasers employed consist of an oscillator plus one stage of amplification, transversely pumped by the second harmonic of a pulsed $(5Hz)$ NdYAG laser, delivering pulses of $\sim 10nsec$ and 20kW peak power. The oscillators were operated with a grazing incidence grating in the range of 560-640nm with linewidths of $\sim 0.5cm^{-1}$. The dye laser beams were spatially overlapped by a dichroic mirror (DM) forming a bichromatic beam of frequencies ω_1 and ω_2. The bichromatic beam is split in two by a beam splitter (BS) and recombined through a lens (L) after being properly delayed to form a small ($\sim$ 8 mrad) angle at the sample position. As indicated in Fig.1 the two parallel polarized beams produce a self-diffracted signal in either direction $(2\vec{k}^{(1)} - \vec{k}^{(2)})$ or $(2\vec{k}^{(2)} - \vec{k}^{(1)})$. The lenses in front of the $0.25m$ monochromators collect the generated signals and focus them in the entrance slits. The apertures along the beam path are essential to reduce the background noise due to the scattered light. Both signals were detected through monochromators equipped with photomultipliers and processed with a boxcar averager or a microcomputer.

Cornrnercially available serniconductor doped glasses (SDG), manufactured by Corning Glass, were used in our experiments.

In a typical run, the signals in both directions were recorded as the relative time delay between the two bichromatic beams is changed using a variable delay line. The monochromators were used to select one of the frequency components. Fig.2 illustrates the diffracted signal intensity at frequency ω_1 as a function of the time delay. The $\sim 19fs$ oscillation period corresponds to the inverse of the frequency separation $(\omega_1 - \omega_2/2\pi)$ of the lasers used. The behavior of the signal at frequency ω_2 is analogous. The relative phase ϕ_i of the signals is a function of $\left(\frac{\hbar\omega_i}{E_g}\right)$, i = 1, 2, where E_g is the SDG energy gap which has a different value for each CdS_xSe_{1-x} sample composition.

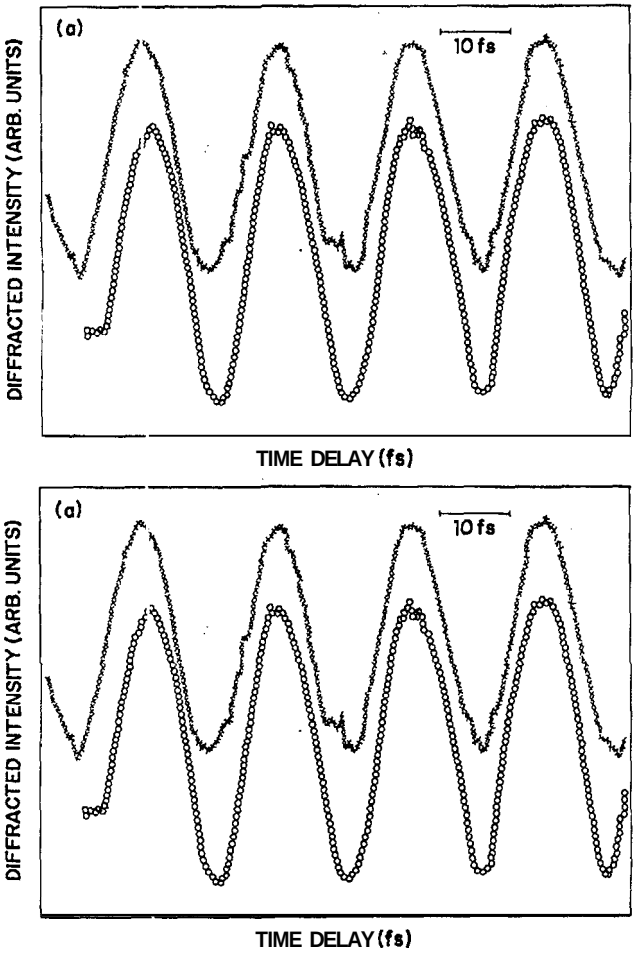

Figure 2: Recorded diffracted intensities observed at frequency ω_1 veisus the time-delay for a bichromatic beam with wavelengths $\lambda_1 = 532nm$ and $\lambda_2 = 588nm$: a) $\phi_1 \sim 2°$, sample CS 3-69: b) $\phi_1 \sim 33°$, sample: CS 3-67. The traces illustrrate the signals emitted along the two directions corresponding to $2\vec{k}^{(1)} - \vec{k}^{(2)}$ and $2\vec{k}^{(2)} - \vec{k}^{(1)}$. (The figures are vertically displaced for clarity.)

The CdS_xSe_{1-x} doped glasses (3mm thickness) studied are indicated in Table I with the relevant parameters. The laser frequency ω_2 was smaller than the samples band gap frequencies as illustrated by the negative values of $(\omega_2 - \omega_g)T_2$. For all those values $Im\chi^{(3)}(\omega_2, \omega_2, \omega_2, -\omega_2) = 0$ as shown previously[8,9].

Two series of measurements were performed to measure ϕ_1 and ϕ_2, respectively. In the first one we observed the signal component at the frequency ω_1 using Corning glass samples CS 3-69, CS 3-67 and CS 2-61. For all samples we expect that $Im\chi^{(3)}(\omega_1, \omega_1, \omega_2, -\omega_2) = 0$ because the absorption of I_1 should not be influenced by I_2 whose frequency is smaller than ω_g. Then in this case ϕ_1 represents the phase of $\chi^{(3)}(\omega_1, \omega_1, \omega_1, -\omega_1)$ which depends on $(\omega_1 - \omega_g)T_2$ as indicated in Table I. For the glass CS 3-69 the value $\phi_1 = 2°$ is in agreement with our expectation since large frequency detunings of ω_1 and ω_2 from the energy gap were used. A similar result was obtained for the sample CS 2-61 when ω_1 and ω_2 were simultaneously smaller than ω_g. On the other hand, changes of ϕ_1 were observed for the glasses CS 3-67 and CS 2-61 corresponding to $\omega_1 > \omega_g$ and $\omega_2 < \omega_g$. In the second set of measurements we observed the signal component at frequency ω_2 using samples CS 3-69, CS 3-67 and CS 3-66 in order to rneasure ϕ_2. Since $Im\chi^{(3)}(\omega_2, \omega_2, \omega_2, -\omega_2) = 0$, ϕ_2 represents the phase of $\chi^{(3)}(\omega_2, \omega_1, \omega_2, -\omega_1)$ as indicated in Table I. For the laser wavelengths employed we observed changes of ϕ_2 that correspond to different values of $(\omega_1 - \omega_g)$ detuning. Unfortunately no previous results are available to make comparison with our measurements. However, we attribute the observed frequency dependence of $\chi^{(3)}(\omega_2, \omega_1, \omega_2, -\omega_1)$ to the effect of the field at ω_1, which influences the transmission of the other frequency component and causes bandfilling in the conduction band or saturation of the trapping-states. This assumption is corroborated by other experiments with SDG. On the other hand, the observed frequency dispersion of the degenerate $\chi^{(3)}$ shows a qualitative agreement with the predictions of the electronic bandfilling model as in the previous experiments[8,9].

A comparison with the experimental methods of other authors is appropriate at this point. In refs. [8] and [9], Roussignol and co-workers measured the phase of degenerate $\chi^{(3)}$ in phase-conjugation experiments using a delicate technique that requires transform-limited pulses, a perfect control of the laser frequency chirp, and accurate intensity measurements. Other researchers used interferometric methods to determine the phase of the degenerate nonlinear susceptibility (see ref.[17] for previous work). It seems very difficult to obtain information on the nondegenerate $\chi^{(3)}$ with those methods. We note' that, contrary to the other methods, the one reported herein does not require an absolute measurement of beam intensities, and non-transform-limited pulses can also be used. Furthermore the present method does not require the use of a reference sample. One lirnitation of our method

Table i. Survey of the experimental parameters. ω_g is the optical frequency corresponding to 1% transmission and E_g is the corresponding energy. T_2 is the dephasing time assumed to be 20 fs. The maximum error in the angles ϕ_1 and ϕ_2 was estimated to be $\pm 5°$.

Corning Glass Filter	$E_g(eV)$	$(\omega_1-\omega_g)T_2$	$(\omega_2-\omega_g)T_2$	ϕ_1	$\frac{Im\,\chi^{(3)}(\omega_1,\omega_1,\omega_1,-\omega_1)}{Re\,\chi^{(3)}(\omega_1,\omega_1,\omega_1,-\omega_1)}$	ϕ_2	$\frac{Im\,\chi^{(3)}(\omega_2,\omega_1,\omega_2,-\omega_1)}{Re\,\chi^{(3)}(\omega_2,\omega_1,\omega_2,-\omega_1)}$
CS 3-69	2.43	-3.2	-10.6	2°	0.03	5°	0.09
CS 3-67	2.28	+3.6	-3.2	33°	0.65	13°	0.23
CS 3-66	2.22	+3.6	-3.2			17°	0.30
		-2.0	-0.4	0°	0		
CS 2-61	2.05	+1.0	-2.0	14°	0.25		
		+2.0	-2.0	28°	0.53		

at the present stage results from the experimental arrangement that does not allow a larger accuracy, but an improvement in the electronic data processing will provide a significant reduction of the relative errors in future applications.

b. Measurements of the phase of $\chi^{(5)}$

For highly nonlinear media such as semiconductors, polymers or special glasses, high-order nonlinearities may also contribute at moderate intensity levels. For example, Maruani et al. have studied high-order nonlinearities in $CuC\ell$ using self-diffraction in a non-phase-matched scheme[27]. Acioli et al. reported direct measurements of $|\chi^{(5)}|$ and $|\chi^{(7)}|$ in semiconductor doped glasses in a phase-matched multiwave-mixing configuration[28]. More recently, Charra et al.[29] reported on non-degenerate multiwave mixing in polydiacetylene through phase-conjugation with frequency conversion. Nevertheless, although a number of reports are concerned with the measurements of $|\chi^{(n)}|$, n > 3, no technique has been developed to measure the phase of high-order susceptibilities.

In this section, we show how the polarization beats spectroscopy can be used to measure the phase of $\chi^{(5)}$ in a solid and review our own results obtained using this new technique[20].

The principle of the experiment is similar to the one introduced in Sec.II.a. However, in this case we have to be carefull because of possible competing effects as discussed below. Although the intensity of the beam diffracted at the first-order is contributed primarily by $\chi^{(3)}$, the second-order diffraction signal may include contributions from $\chi^{(5)}$ and cascade processes due to $\chi^{(3)}$. Let us assume here that the cascade contribution is negligible as compared to that of the direct fifth-order nonlinearity. Thus, the signal beam at ω_1 emitted along the direction $3\vec{k}^{(1)} - 2\vec{k}^{(2)}$ is generated by the polarization $P^{(5)}(\omega_1) = P_A^{(5)}(\omega_1) + P_B^{(5)}(\omega_1) + P_C^{(5)}(\omega_1)$ with

$$\begin{aligned} P_A^{(5)}(\omega_1) &= \chi_A^{(5)}(\omega_1,\omega_1,-\omega_1,\omega_1,-\omega_1,\omega_1)\left[E_1^{(1)}(E_1^{(2)})^*\right]^2 E_1^{(1)} \\ &\times \exp\left\{i\left[2\left(\vec{k}_1^{(1)}-\vec{k}_1^{(2)}\right)\cdot\vec{r}+2\omega_1\tau+\vec{k}_1^{(1)}\cdot\vec{r}-\omega_1 t+\theta_1\right]\right\} \quad , \qquad (6) \\ P_B^{(5)}(\omega_1) &= \chi_B^{(5)}(\omega_1,\omega_2,-\omega_2,\omega_2,-\omega_2,\omega_1)\left[E_2^{(1)}(E_2^{(2)})^*\right]^2 E_1^{(1)} \\ &\times exp\left\{i\left[2\left(\vec{k}_2^{(1)}-\vec{k}_2^{(2)}\right)\cdot\vec{r}+2\omega_2\tau+\vec{k}_1^{(1)}\cdot\vec{r}-\omega_1 t+\theta_1\right]\right\} \quad , \qquad (7) \\ P_C^{(5)}(\omega_1) &= \chi_C^{(5)}(\omega_1,\omega_1,-\omega_1,\omega_2,-\omega_2,\omega_1)E_1^{(1)}(E_1^{(2)})^*E_2^{(1)}(E_2^{(2)})^*E_1^{(1)} \\ &\times \exp\left\{i\left[\left(\vec{k}_1^{(1)}-\vec{k}_1^{(2)}+\vec{k}_2^{(1)}-\vec{k}_2^{(2)}\right)\cdot\vec{r}+(\omega_1+\omega_2)\tau+\vec{k}_1^{(1)}\cdot\vec{r}-\omega_1 t+\theta_1\right]\right\}, \qquad (8) \end{aligned}$$

where r is the relative time-delay between the two bichromatic beams. The signal intensity at ω_1, proportional to $|P^{(5)}(\omega_1)|^2$, is given by

$$I(\omega_1) \propto a + b\cos(2\Delta\vec{k}\cdot\vec{r} + 2\omega_M\tau + \phi_1) + c\cos(\Delta\vec{k}\cdot\vec{r} + \omega_M\tau + \phi_2) + d\cos(\Delta\vec{k}\cdot\vec{r} + \omega_M\tau + \phi_3) = a + b\cos(2\Delta\vec{k}\cdot\vec{r} + 2\omega_M\tau + \phi_1) - c'\cos(\Delta\vec{k}\cdot\vec{r} + \omega_M\tau + \phi'), \quad (9)$$

where

$$a = \left|\chi_A^{(5)}[E_1^{(1)}(E_1^{(2)})^*]^2\right|^2 + \left|\chi_B^{(5)}[E_2^{(1)}(E_2^{(2)})^*]^2\right|^2 + \left|\chi_C^{(5)}E_1^{(1)}(E_1^{(2)})^*E_2^{(1)}(E_2^{(2)})^*\right|^2;$$

$$b = 2\left|\chi_A^{(5)}\chi_B^{(5)}[E_1^{(1)}(E_1^{(2)})^*]^2[E_2^{(1)}(E_2^{(2)})^*]^2\right|;$$

$$c = 2\left|\chi_A^{(5)}\chi_C^{(5)}[E_1^{(1)}(E_1^{(2)})^*]^3E_2^{(1)}(E_2^{(2)})^*\right|;$$

and

$$d = 2\left|\chi_B^{(5)}\chi_C^{(5)}E_1^{(1)}(E_1^{(2)})^*[E_2^{(1)}(E_2^{(2)})^*]^3\right|;$$

$$\Delta\vec{k} = \vec{k}_1^{(1)} - \vec{k}_1^{(2)} - (\vec{k}_2^{(1)} - \vec{k}_2^{(2)});$$

$\omega_M = \omega_1 - \omega_2$ is the modulation frequency; $\phi_1 = \phi_A - \phi_B$, $\phi_2 = \phi_A - \phi_C$ and $\phi_3 = \phi_B - \phi_C$, with $\phi_A = arc\ tan\left[Im\,\chi_A^{(5)}/Re\,\chi_A^{(5)}\right]$, $\phi_B = arc\ tan\left[Im\,\chi_B^{(5)}/Re\,\chi_B^{(5)}\right]$ and $\phi_C = arc\ tan\left[Im\ \chi_C^{(5)}/Re\,\chi_C^{(5)}\right]$; $c' = [(c\cdot cos\,\phi_2 + d\cdot cos\phi_3)^2 + (c\ sin\phi_2 + d\ sin\phi_3)^2]^{1/2}$ and $\phi' = arc\sin[(c.\,sin\phi_2 + d.\,sin\phi_3)/c']$ which is intensity dependent.

Eq.(9) shows that the second-order diffraction signals have Fourier components at ω_M and $2\omega_M$. Analogous calculations for $I(\omega_1)$ emitted along the direction $3\vec{k}^{(2)} - 2\vec{k}^{(1)}$ provide a similar signal with Fourier components which are $(-2\phi_1)$ and $(-24')$ out-of-phase with the signals indicated in eq.(9). Consequently, if the signals in both directions are simultaneously recorded in two independent detectors, one may obtain information on ϕ_1 and ϕ' using the following steps. First, the relative amplitudes of b and c' can be determined by Fourier analysis. Then, ϕ_1 and ϕ' can be obtained by fitting the shapes of the modulated signals and the relative phase-shift between the signals at both directions. Using the appropriate laser wavelengths to cancel ϕ_A or ϕ_B, the value of one of them can be calculated from ϕ_1, in a manner which is similar to the determination of the phase of $\chi^{(3)}$.

To study the phase of $\chi^{(5)}$ in commercial SDG we first note that cascade contributions from the lower order nonlinearities are negligible in comparision with that of the direct higher-order nonlinearity for the reasons discussed below. To estimate the contribution of the cascade process due to $\chi^{(3)}$ we have used the diffraction theory developed by Klein and Cook[30]. The equation describing the amplitude of the diffracted optical fields is obtained from the optical wave equation,

$$\nabla^2 E_i = \frac{[\mu(x)]^2}{c^2}\frac{\partial^2 E_i}{\partial t^2}, \quad (10)$$

where the refractive index in the region where the beams overlap $(0 < z < L)$ is given by

$$\mu(x) = \mu_0 + \mu_1 \sin(k^* x) \quad , \quad (11)$$

where $k^* = 2\pi/\Lambda$ is the wavenumber of the refractive grating and $A = \lambda_e/2\ sin\ 8$, with λ_e being the wavelength of the pump beams. The basic equation is obtained from (10) and (11) introducing the electric field $E_i = \sum_{n=-\infty}^{+\infty}\phi_n(z)\,exp\,i(\omega_i t - \vec{k}_n\cdot\vec{r})$ into the wave equation and neglecting second order terms which include $\nabla^2\phi_n(z)$ and μ_1^2. Then, we obtain

$$\frac{d\phi_n}{dz} + \frac{v}{2L}(\phi_{n-1} - \phi_{n+1}) = i\frac{nQ}{2L}(n - 2\alpha)\phi_n, \quad (12)$$

where $Q = k^{*2}L/\mu_0 k$ with k^*, L, μ_0 and k being the grating wavenumber, sample thickness, refractive index and diffracted beam wavenumber. $v = k\mu_1 L$ is the modulation depth and μ_1 is the first-order Fourier component of the refractive index. The parameter $a = -(\mu_0 k/k^*)sin\theta$ is a geometry dependent quantity where θ is the half intersection angle between the incident beams. The self-diffraction case corresponds to $\alpha = -1/2$. Hence, once a is set, the diffraction efficiencies are determined by the parameter Q which represents phase-mismatch, and the modulation depth v. For $v \ll 1$, we may solve eq.(12) by using the approximation $|\phi_{n+1}| \ll |\phi_n|$ for $n \geq 0$ and $|\phi_{n-1}| \ll |\phi_n|$ for $n \leq 0$. For the first-order self-diffracted beam intensity we have:

$$I_1 = \left(\frac{v}{Q}\right)^2 I_0 sin^2\left(\frac{Q}{2}\right) \overset{Q\to 0}{=} \left(\frac{v}{2}\right)^2 I_0 \quad , \quad (13)$$

where I_0 is the incident laser intensity. For the second-order diffraction beam we obtain

$$I_2 = \left(\frac{v^4}{16Q^4}\right) I_0 \left\{\left[\frac{1 - cos(3Q)}{3} - \frac{1 - cos(2Q)}{2}\right]^2 + \left[\frac{sin(3Q)}{3} - \frac{sin(2Q)}{2}\right]^2\right\} \overset{Q\to 0}{=} \left(\frac{v^4}{64}\right) I_0. \quad (14)$$

Therefore, measuring the relative intensities of the zero and first-order diffracted beams, we may determine the cascade contribution using eqs.(13) and (14). Experimentally, one can measure the relative intensity of the second-order diffracted beam which has both contributions from the direct fifth-order nonlinearity and the

cascade process. Thus, it is possible to determine the relative contribution between $\chi^{(5)}$ and $[\chi^{(3)}]^2$. In our experiments, we have measured those three relative intensities at different laser wavelengths (including degenerate and nondegenerate cases) and for different intensities used. The results show that the calculated cascade contributions are at least one order of magnitude smaller than the measured second-order diffracted beam intensities. Also the results show that for the higher intensities used, the contribution from the direct fifth-order nonlinearity is increased.

It should be pointed out that, when the contribution of the direct fifth-order nonlinearity is close to or even less than the cascade contribution, the phase-matched higher-order diffraction geometry should be used. For that geometry, the diffracted beams due to the direct higher-order nonlinearity are the higher-order Bragg-reflections with phase-match, while cascade contributions become negligible because of the phase-mismatch. This was considered in the ref. [31].

The experimental setup used was the same used for rneasuring the phase of $\chi^{(3)}$ (Fig.1).

The sample used was a $Cd(S,\mathrm{Se})$ doped Corning glass CS 2-73 with energy gap of $2.17eV$ which corresponds to 1% transmission. To perform the experiments we set $\omega_1 < E_g/\hbar$ because we expect that $Im\chi_A^{(5)} = 0$ for a large frequency detuning from the band gap.

Fig.3 shows the recorded signals in both directions as the relative time-delay between the two bichromatic beams was changed. Fig.3(a) and 3(b) show that, for the same laser frequencies, the signals are intensity dependent. Note that at relatively low powers the signals in Fig.3(a) have Fourier components at ω_M and $2\omega_M$ as predicted from eq.(9). For large powers, as in Fig.3(b), the component at $2\omega_M$ is reduced and then the information on the phase ϕ_1 is lost. This is explained using eqs.(6-9) which show that the Fourier component at $2\omega_M$ becomes negligible if one of the products $|P_A P_C|$ and $|P_B P_C|$ is much larger than $|P_A P_B|$. For $\omega_2 > \omega_1$, $\chi_A^{(5)}$ and $\chi_C^{(5)}$ will decrease with the increase of $I(\omega_2)$ due to the optical switch effect[33]. However, $\chi_C^{(5)}$ is expected to decrease less than $\chi_A^{(5)}$ so that the Fourier component at $2\omega_M$ decreases as compared to the component at ω_M. Meanwhile, this intensity dependent result may also be affected by higher-order nonlinearities at the intensities used[28]. For example, the second-order diffracted signals may include contributions due to $\chi^{(7)}$ and thus the information on $\chi^{(5)}$ could be masked. Therefore, one should work at relatively weak excitations so that $\chi^{(5)}$ plays a dominant role and the optical switch effect does not becomes important. In the present experiment the $2\omega_M$ component appears for the incident intensities indicated in Fig.3(a) and

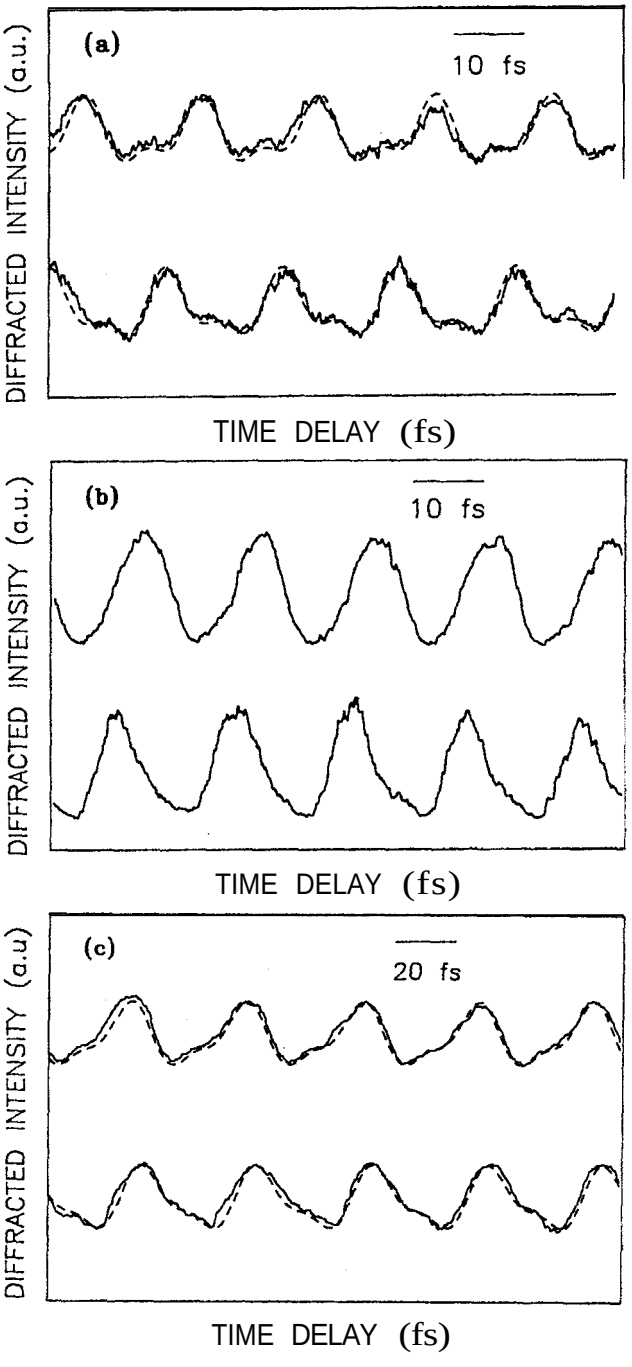

Figure 3: The solid lines illustrate the recorded second-order diffracted signals as a function of the time delay. The dashed lines were calculated from eq.(9) as explained in the text. (Sample: Corning glass CS 2-73, 3mm thickness). (a) $\hbar\omega_1 = 2.03eV$, $\hbar\omega_2 = 2.21eV$, $I(\omega_1) = 0.3MW/cm^2$, $I(\omega_2) = 0.1MW/cm^2$; (b) the same frequencies used as in (a) but $I(\omega_1) = 12MW/cm^2$, $I(\omega_2) = 4MW/cm^2$; (c) $\hbar\omega_1 = 2.03eV$, $\hbar\omega_2 = 2.14eV$, $I(\omega_1) = 0.2\mathrm{MW/cm^2}$, $I(\omega_2) = 10KW/cm^2$.

smaller values. Although the signals at these conditions are close to our detection limit, ϕ_1 could be deduced by fitting the experimental data with the formula given in eq.(9). The obtained value was $\phi_1 = 60°$ with ratio $c'/b = 0.5$. The fitting error is about 20°. Finally, as-

suming that $Im\,\chi_A^{(5)} = 0$ for $(\hbar\omega_1 - E_g) = -0.14eV$, we determined the phase of $\chi_B^{(5)}(\omega_1, \omega_2, -\omega_2, \omega_2, -\omega_2, \omega_1)$ to be $60° \pm 20°$ after averaging several measurements.

Fig.3(c) corresponds to the case where ω_1 and ω_2 are smaller than $E_g/\hbar$. In this case the value obtained for ϕ_1 was $8° \pm 20°$ with the ratio $c'/b = 0.35$, which supports our assumption that $Im\,\chi^{(5)} = 0$ if all the related freqiiencies are smaller than $E_g/\hbar$. Also in this case if we increase the laser intensities, the component at $2\omega_M$ disappears.

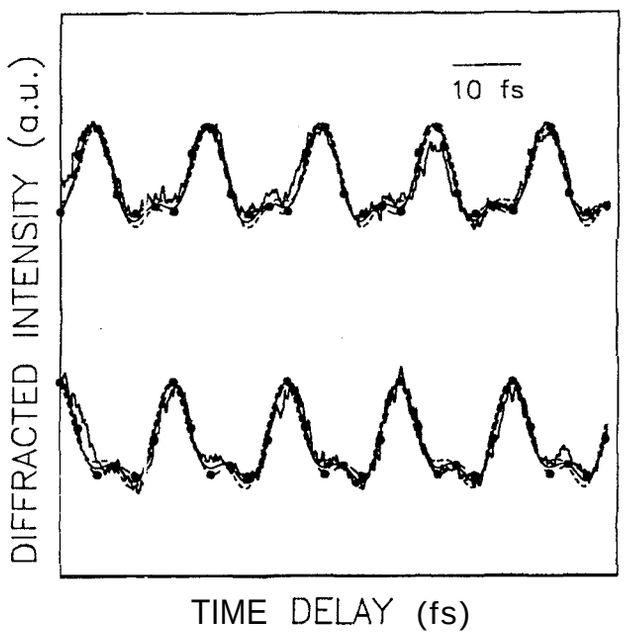

Figure 4: Comparison between the experimental data shown in Fig.3(a) and the theoretical predictions of eq.(9) for different fitting parameters. $(-\bullet-)$ $\phi_1 = \phi - 20°$; (——) $\phi_1 = 9$; $(--)$ $\phi_1 = \phi +$ [illegible]

In order to determine the limitations of the technique in the measurement of ϕ_1, we present in Fig.4 the results of the theoretical fitting of the modulated signal for diflèrent fitting parameters.

We note that for relatively large changes of the theoretical values for ϕ_1, on the order of 20 degrees, there is not a very large change of the resulting fits. From this we concludec that this method is not as precise as in the previous case (Sec.II.a) to determine the dispersion of the high-order nonlinear optical susceptibility. This problem is due to contribution of the first-order Fourier component in the recorded modulation signals and can possibly be circunvented if better detection schemes are employed in order to use lower intensities in the incident bearns.

To understand the significance of the phase-angles obtained we have performed a calculation using the bandfilling model[9] assuming that the traps levels are saturated. While in ref.[9] $\chi^{(3)}$ was deduced from the slope of the total susceptibility χ versus the laser intensity $\mathbf{I}$ at low excitation levels, in our case, since the effective polarization for the second-order diffraction was intensity dependent, we considered that $\mathbf{I} = I_0 + I_1 cos(\delta kx)$, where x is the ordinate along the grating direction and $\delta\vec{k} = \vec{k}^{(1)} - \vec{k}^{(2)}$ I_0 and $I_1 (I_0 \geq I_1)$ are intensities of background and modulation, respectively. We could calculate the total χ and the effective susceptibility responsible for the second-order diffraction signal was obtained from $\chi_{eff}^{(5)} = \frac{1}{2\pi}\int_0^{2\pi} \chi\, cos(2\delta kx)\, d(6k.x)$.

The procedure to calculate the nonlinear susceptibility is described in what follows. The first step is to calculate the carrier density, n, created by the incident beams. This is done using a rate equation for n and the result in the case of a relaxation time that is fast as compared to the pulse duration is

$$n = \frac{\alpha(I)I}{\hbar\omega}\tau, \tag{15}$$

where α is the absorption coefficient, $\mathbf{I}$ is the laser intensity, and τ is the pulse duration. From this result it is possible to calculate the position of the quasi-Fermi level of the electrons in the conduction band. The occupation number of the holes can be neglected in the calculations due to the larger effective mass of the valence band. Assuming parabolic band-structure, the expression for the nonlinear susceptibility $\chi(\omega, \mathrm{I})$ is given by

$$\chi(\omega, I) = \left|\frac{er_{cv}}{\pi}\right|^2 \int_0^\infty \frac{1 - \rho_e(k)}{\omega - \omega_{cv}(k) - i\Gamma_{cv}} g(k)k^2 dk, \tag{16}$$

where e is the electron charge, $\rho_e(k)$ is the electron occupation probability factor, r_{cv} is the dipole moment of the valence to conduction band transition, assumed to be constant, $\omega_{cv}(k) = \hbar k^2/2m^* + E_g$, is the energy separation of the optically connected states, Γ_{cv} is the dephasing rate of the transition, and $m^* = (1/m_c + 1/m_v)^{-1}$ is the reduced mass. It has been introduced an ad hoc broadening of the transition line shape given by $g(k)$, following Roussignol et al.[9], and also proposed by Banyai and Koch[34].

Combining the results of eq. (16) for $\chi(\omega, \mathbf{I})$ with the one for $\chi_{eff}^{(5)}$ it is possible to obtain the ratio of the imaginary and real parts of this effective susceptibility, that is, its phase. The calculated phase-angle for the conditions of Fig.3(a) was 70° in agreement with the experiment. The theory also shows that: (i) for excitation levels close to the values used in the experiment, the phase of $\chi_{eff}^{(5)}$ is intensity dependent; (ii) for laser frequencies smaller than $E_g/\hbar$ the phase of the degenerate $\chi_{eff}^{(5)}$ is close to 0°.

III. Conclusions

The method herein presented is quite general and can be readily applied to a large variety of materials. For the case of the third order susceptibility an extension lias already been reported for measuring its phase

dispersion close to a Raman resonance[18]. Further extensions may also include the study of the phase dispersion of $\chi^{(3)}$ in the vicinity of a two-photon absorption resonance. For the study of high-order nonlinear susceptibilities it has been shown that the applicability of the method to the particular case of $\chi^{(5)}$ is dependent on the ratio between the two Fourier components which contribute to the second order diffracted signals. Finally, we note that in both cases described above this technique can be extended, by choosing appropriately the polarizations of the incident beams, to study the various tensor components of the nonlinear susceptibilities.

Acknowledgements

This research was supported in part by the Brazilian agencies: Conselho Nacional de Desenvolvimento Científico e Tecnológico (CNPq), Financiadora de Estudos e Projetos (FINEP) and Fundação de Amparo à Ciência e Tecnologia de Pernambuco (FACEPE). We also thank Luís E.E. de Araújo for help with the data acquisition system.

References

1. N. Bloembergen, *Nonlinear Optics* (Benjamin, Reading, 1965).
2. P. N. Butcher and D. Cotter *The Elements of Nonlinear Optics* (Cambridge U. Press, Cambridge, 1990).
3. Y. R. Shen, *The Principles of Nonlinear Optics* (Wiley, New York, 1984).
4. R. Superfine, J. Y. Huang and Y. R. Shen, Opt. Lett. 15, 1276 (1990).
5. W. Margulis, I. C. S. Carvalho and J. P. von der Weid, Opt. Lett. 14, 700 (1989).
6. J. K. Koch and G. T. Moore, Opt. Lett. 16, 1436 (1991).
7. M. D. Levenson, *Introduction to Nonlinear Laser Spectroscopy* (Academic, New York, 1982).
8. F. Hache, P. Roussignol, D. Ricard and C. Flytzanis, Opt. Commun. 64, 200 (1987).
9. P. Roussignol, D. Ricard and C. Flytzanis, Appl. Phys. A 44, 285 (1987).
10. R. T. Lynch Jr. and H. Lotem, Phys. Rev. Lett. 37, 334 (1976).
11. H. Lotem, R. T. Lynch Jr. and N. Bloembergen, Phys. Rev. A **14**, 1748 (1976).
12. R. T. Lynch Jr. and H. Lotem, J. Chem. Phys. 66, 1905 (1977).
13. D. DeBeer, L. G. VanWagenen, R. Beach and S. R. Hartmann, Phys. Rev. Lett. 56, 1128 (1986).
14. J. E. Rothenberg and D. Grischkowsky, Opt. Lett. 10, 22 (1985).
15. V. L. Bogdahov, A. B. Evdokinov, G. V. Lumonskii and B. D. Fainberg, JETP Lett. 49, 157 (1989); W. Li, H. G. Purucker and A. Lauberau, Opt. Commun. 94, 300 (1992).
16. L. H. Acioli, A. S. L. Gomes and Cid B. de Araújo, Electron. Lett. 26, 92 (1990).
17. H. Ma, L. H. Acioli, A. S. L. Gomes and Cid B. de Araújo, Opt. Lett. 16, 630 (1991).
18. H. Ma, A. S. L. Gomes and Cid B. de Araújo, Opt. Lett. 17, 1052 (1992).
19. H. Ma, A. S. L. Gomes and Cid B. de Araújo, Opt. Commun. 90, 7 (1992).
20. H. Ma, Luís E. E. de Araújo, A. S. L. Gomes and Cid B. de Araújo, *Phase Measurement of the Fifth-Order Susceptibility of Cd(S,*Se*) Doped Glasses,* to be published.
21. H. Ma, A. S. L. Gomes and Cid B. de Araújo, Appl. Phys. Lett. 59, 2666 (1991).
22. M. Sheik-Bahae, J. Wang, R. DeSalvo, D. J. Hagan and E. W. Van Stryland, Opt. Lett. **17**, 258 (1992).
23. J. M. Hickmann, A. S. L. Gomes and Cid B. de Araújo, Phys. Rev. Lett. 68, 3546 (1992).
24. A. J. Stentz, M. Kauranen, J. J. Maki, G. P. Agrawal and R. W. Boyd, Opt. Lett. 17, 19 (1992).
25. R. dela Fuente and A. Barthelemy, IEEE J. Quantum Electron. **28,** 547 (1992).
26. G. G. Luther and C. J. McKinstrie, J. Opt. Soc. Am. B 9, 1047 (1992).
27. A. Maruani, J. L. Oudar, E. Batifol, and D. S. Chemla, Phys. Rev. Lett. 41, 1372 (1978).
28. L. H. Acioli, A. S. L. Gomes and J. R. Rios Leite, Appl. Phys. Lett. 53, 1788 (1988).
29. F. Charra and J. M. Nunzi, J. Opt. Soc. Am. 8, 570 (1991).
30. W. R. Klein and B. D. Cook, IEEE Trans. Sonics and Ultrasonics SU-14, 123 (1967).
31. H. Ma, A. S. L. Gomes and Cid B. de Araújo, *"Cascade Contributions in High-Order Optical Nonlinearity Measurements"* Opt. Comm. (1993).
32. C. Flytzanis, F. Hache, M. C. Klein, D. Ricard and P. Roussignol, in *Progress in Optics,* E. Wolf ed. (North-Holland, Amsterdam, 1991). Vol. XXIX, p.321.
33. H. Ma, A. S. L. Gomes and Cid B. de Araújo, Opt. Lett. 18, (March, 1993).
34. L. Banyai and S. W. Koch, Z. Phys. B 63, 283 (1986).